



HAL
open science

Stray light estimates due to micrometeoroid damage in space optics, application to the LISA telescope

V. Khodnevych, Michel Lintz, Nicoleta Dinu-Jaeger, Nelson Christensen

► **To cite this version:**

V. Khodnevych, Michel Lintz, Nicoleta Dinu-Jaeger, Nelson Christensen. Stray light estimates due to micrometeoroid damage in space optics, application to the LISA telescope. *Journal of Astronomical Telescopes Instruments and Systems*, 2020, 6 (4), pp.048005. 10.1117/1.JATIS.6.4.048005 . hal-03064405

HAL Id: hal-03064405

<https://hal.science/hal-03064405>

Submitted on 14 Dec 2020

HAL is a multi-disciplinary open access archive for the deposit and dissemination of scientific research documents, whether they are published or not. The documents may come from teaching and research institutions in France or abroad, or from public or private research centers.

L'archive ouverte pluridisciplinaire **HAL**, est destinée au dépôt et à la diffusion de documents scientifiques de niveau recherche, publiés ou non, émanant des établissements d'enseignement et de recherche français ou étrangers, des laboratoires publics ou privés.

1 Stray light estimates due to micrometeoroid damage in space optics, 2 application to the LISA telescope

3 **Vitalii Khodnevych^{a,b,*}, Michel Lintz^{a,b}, Nicoleta Dinu-Jaeger^{a,b}, Nelson Christensen^{a,b}**

4 ^aArtemis, Observatoire Côte d'Azur, CNRS, CS 34229, 06304 Nice Cedex 4, France

5 ^bUniversité Côte d'Azur, 28 Avenue Valrose, Nice, France, 06100

6 **Abstract.** The impact on an optical surface by a micrometeoroid gives rise to a specific type of stray light inherent
7 only in space optical instruments. This causes a double source of light scattering: the impact crater, and the ejected
8 contamination. We propose a method of stray light estimation and apply it to the case of the Laser Interferometer
9 Space Antenna (LISA) telescope. We estimate the backscattering fraction for nominal (4 years) and extended (10
10 years) mission durations.

11 **Keywords:** Space optics, Stray light, BRDF, micrometeoroid, LISA.

12 *Vitalii Khodnevych, vitalii.khodnevych@oca.eu

13 1 Introduction

14 Scattering due to micrometeoroid damage is a specific type of stray-light, which is inherent only in
15 space instruments with optics exposed to the space environment. Free flying dust particles in space
16 can hit and damage the optical surface. These will cause an increase of stray light in the system.
17 The problem of micrometeoroid damage exists since the first space flights.¹ However, only a few
18 papers^{2,3} give an estimate of this type of stray-light. This work aims at improving the simulation of
19 scattered stray light that results from the impact of micrometeoroids in space optical instruments.

20 To estimate light scattering induced by the micrometeoroid damage, we propose a method
21 which consists of four steps:

- 22 1. Definition of the environmental conditions (Particulates Environmental Model) of the satel-
23 lite: estimation of the flux and parameters of the particles which arrive at the critical surfaces.
- 24 2. Calculation of the expected damage crater diameter and ejected mass due to micrometeoroid
25 impact.

26 3. Calculation, with the Peterson model,⁴ of the BSDF that results from the impact craters.
27 Calculation of the corresponding cleanliness level and slope due to contamination by ejected
28 mass.

29 4. Optical software (FRED) calculation of the scattered light.

30 In this paper, we apply this method to the case of the LISA (Laser Interferometer Space Antenna)
31 telescope and consider the sun-orbiting LISA trajectory, 50 Mkm away from the Earth, in the
32 micrometeoroid flux estimates. In the following, each step will be described, and the results will
33 be presented.

34 **2 LISA Instrument**

35 LISA will be the first space-based gravitational waves (GW) observatory.⁵ GW are ripples in space-
36 time generated by the movement of massive objects. Albert Einstein predicted them in 1916.⁶ The
37 first direct observation of GW was made in 2015 by the ground-based interferometer LIGO⁷ in the
38 USA (Nobel Prize 2017). Due to seismic noise, gravity gradient noise, and other effects, ground-
39 based interferometers (LIGO, Virgo) are limited at low frequencies. Significant improvements can
40 be made by the construction of an underground interferometer (Einstein Telescope) on the stable
41 lithospheric plate.⁸ However, even underground detectors will be limited to observing the merger
42 of very compact massive objects, generating a signal at relatively high frequencies. To detect GW
43 at lower frequencies, and detect more massive and slower objects, the detector has to be in space,
44 and is likely to be a space interferometer mission such as LISA. The LISA frequency band will
45 include GW generated by compact objects captured by supermassive black holes in galactic nu-
46 clei, compact binaries in our galaxy and beyond, binary supermassive black holes, and quantum
47 fluctuations in the early universe.

48 LISA is a GW observatory space mission now in Phase A. It is a constellation of three identical
49 satellites, forming an equilateral triangle of arms-length $L=2.5$ million km. The continuous mea-
50 surement of the light path length $L[1 + h(t)]$ between two test masses reveals the presence of the
51 GW $h(t)$. It is performed via six interferometric heterodyne phase measurements that take place
52 at each end of the triangle arms. In the presence of any light which was not intended to be in the
53 design (stray light), the heterodyne interference can be disturbed. The correct assessment of the
54 stray light, together with the instrument stability, is vital for LISA measurements, which aim at a
55 precision of 10^{-21} in the gravitational wave $h(t)$ strain, that is, in the measurement of the fractional
56 change of the light path length $L[1 + h(t)]$.

57 To make the phase measurements between beams from distant satellites possible, an optical
58 telescope is used for transmission and receiving of the beams. The schema of the LISA telescope
59 is given in Fig. 1. In the NASA design,⁹ it is an afocal Cassegrain telescope, which consists of
60 four mirrors. The mirrors are named in sequential order following the beam from the big entrance
61 aperture: M1 (primary mirror), M2 (secondary mirror), M3, and M4. The current off-axis design
62 provides better performance in terms of diffracted light, in comparison to the on-axis configuration.
63 To provide excellent thermal stability of the telescope, the material of the M1 mirror is chosen to
64 be a Zerodur^(R) with a silver coating.

65 The telescope is a part of the MOSA (moving optical sub-assembly), which includes also the
66 optical bench and the gravitational reference sensor. From the optical bench, the transmitted beam
67 propagates through the telescope, and is sent to the distant satellite. The same telescope is used for
68 collecting the received beam. On the optical bench, part of the transmitted beam is pinched off and
69 used for the interference with the received beam. The phase of the interferometric signal encodes
70 information about the gravitational waves $h(t)$.

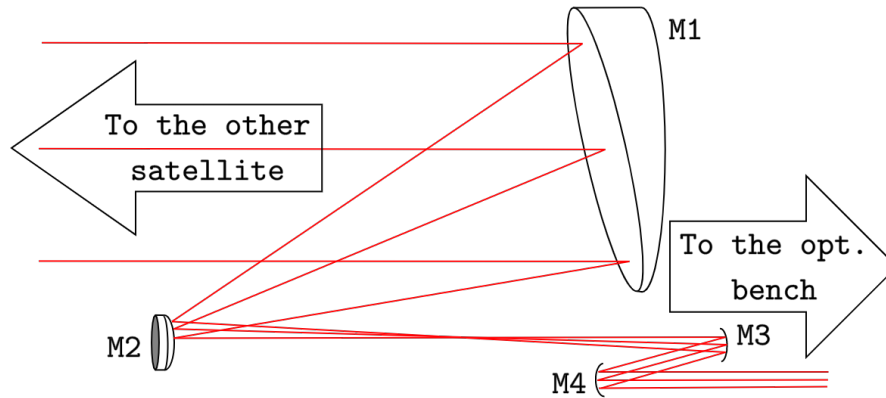


Fig 1 Schema of the Cassegrain four mirror telescope designed by NASA for the LISA mission. The same telescope is used to expand the transmitted beam and collect the light of the received beam.

71 A thermal shield will surround the mirrors of the telescope, and only mirror M1 will be exposed
 72 to the space environment.

73 **3 Stray Light Problem in the LISA Telescope**

74 In the presence of stray light, the phase measurements can be disturbed. The stray light can be con-
 75 sidered as an additional beam if it has the same polarization and optical frequency as the reference
 76 beam. Stray light in LISA includes exterior contributions (stars, planets, etc.), diffraction of the
 77 beam, multiple reflections in optics ("ghosts"), and scattering of the nominal beams. The sources
 78 of scattering are:

- 79 1. Surface microroughness
- 80 2. Contamination: particle, molecular, biological on the surface and in the volume
- 81 3. Cosmetic defects: digs, scratches either due to the assembling of the optical components or
 82 resulting from the impact of micrometeoroids
- 83 4. Backscattering in the optical fibers

84 A common way to describe scattering is the usage of the Bidirectional Scattering Distribution
85 Function (BSDF), which designates how the scattering probability depends on the scattering an-
86 gles. BSDF is the radiance of the scattering surface normalized by the irradiance of the surface.¹⁰
87 BSDF is used by optical software (FRED,¹¹ Zemax,¹² Code V¹³) to perform stray light simulations.
88 When optical and mechanical geometries are defined, and optical properties set, then a BSDF is
89 assigned to each surface. Later, each stray light path is identified. To avoid stray light, the opti-
90 cal designs generally use smooth, clean optics (mirrors, beam dumps), black coating for support
91 structures, unique optical designs, baffles, and stops, etc.

92 *3.1 Environmental conditions: particulates environmental model*

93 The first step of stray light analysis due to micrometeoroid damage is to determine the particulate
94 environment for the satellite. This includes information about the flux, velocity, density, mass,
95 directivity of the micrometeoroids. In the particular case of LISA, the environment of the satellite
96 is given in the LISA Environment Specification document.¹⁴ Charter 5 of that document contains
97 information about the micrometeoroid distribution. However, below we discuss a general approach
98 to the solution of the problem.

99 The flux-mass model for meteoroids at one astronomical unit from the Sun has been proposed
100 and presented by Grün et al.¹⁵ (see Fig. 2). It gives the total average meteoroid flux $\phi_G(m)$ (spo-
101 radic+ stream average) in terms of the integral flux (i.e., the number of particles per square metre,
102 per year, of mass larger than or equal to a given mass m , impacting a randomly-oriented flat plate
103 under a viewing angle of 2π). Except for Earth shielding and gravitational effects (which are neg-
104 ligible at the LISA altitude of 50 Mkm), this flux is omnidirectional.¹⁶ The Grün model accounts
105 for averaging over all directions. Beside this, micrometeoroid streams are not considered. This

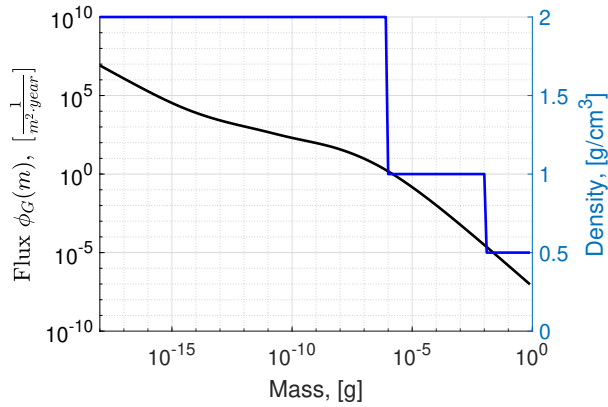


Fig 2 The Grün meteoroid flux-mass model (in black) and the step function of density distribution (in blue)¹⁶

106 interplanetary flux is valid for the micrometeoroid mass range of 1×10^{-18} g to 1 g.

107 For the impact crater calculation, we use a density value of 2.5 g/cm^3 for all ranges of mass,
 108 as was specified in the LISA Environmental model.¹⁴ However, since the mass density of the
 109 micrometeoroids is not a measured quantity, a reasonable assumption should be used instead. An-
 110 other description of the density is given as a function of steps¹⁶ (see fig 2). This function will be
 111 used in Sec. 3.4.

112 As a first approximation, we use the constant value of meteoroid impact velocity 20 km/s for
 113 all the masses of micrometeoroids. This value is the typical mean velocity for a micrometeoroid
 114 impact with a sun-orbiting body,¹⁷ and it is proposed by LISA environmental model.¹⁴

115 The space debris environment is not considered.

116 The next step is to apply this model to the investigated surface. For this, some parameters of
 117 the mission are required: duration of the mission, nature of the critical surfaces (size, material,
 118 orientation, shielding), etc. For the calculation of the number of expected impacts, we use the Grün
 119 model¹⁴ and the following parameters:

- 120 • Nominal mission duration is four years (extended duration is ten years)

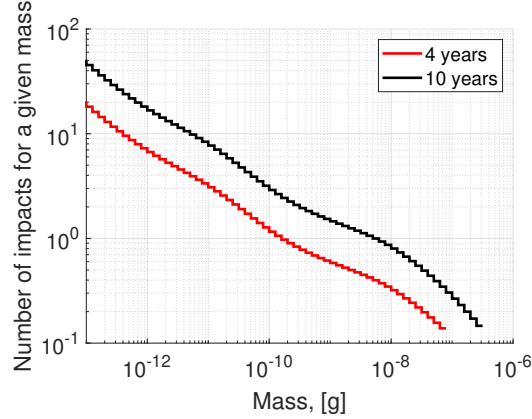


Fig 3 The expected number of micrometeoroid impacts on the M1 mirror, calculated according to the Grün Model, as a function of the micrometeoroid mass. The bin size is logarithmically uniform. The total number of micrometeoroid impacts with mass $> 1 \times 10^{-12}$ g is 92 for four years mission and 231 for ten years mission.

- The primary M1 mirror diameter of the LISA telescope is 0.3 m. We assume that M1 is the only mirror exposed to micrometeoroids.

Because the mechanical structure is unknown at the moment, no correction is made to account for the shielding by the structure surrounding the telescope. The approach presented in this paper corresponds to this worst-case scenario.

Since the flux $\phi_G(m)$ is a cumulative flux, to know the number of expected impacts in a certain mass range (one bin), the difference between neighboring bins should be taken into account. The result of the calculation is given in Fig. 3. The bin size is uniform in the logarithmic scale. The ratio between neighboring bin size is $10^{1/10}$. The number of expected impacts is a fractional value (different from integer²), as it is a statistical quantity. In the mass spectrum of the meteoroid (see Fig. 3), we neglect the high mass tail, for which the cumulated flux is lower than $1/e^2$.

3.2 The effect of the micrometeoroids

The hypervelocity impact of the optical surface causes a double effect in terms of scattering. The direct result of the impact is a micro crater. It causes scattering inside of it and diffraction on the

135 border of the crater. From studies of lunar craters and craters in hardware returned from space, it
136 is known that the shape of the damage crater is approximately circular, independent of microme-
137 teoroid shape or incidence angle.² This is because hypervelocity impact is an explosive release of
138 energy in which heat diffuses outward from a point. In this paper we use a single parameter to de-
139 scribe the impact crater: the Damage Crater Diameter (DCD). Below, we propose several methods
140 to calculate the DCD.

141 Another effect of the hypervelocity impact is the contamination of the surface by the ejected
142 material. There is experimental evidence that ejection takes place, due to the strength of the hy-
143 pervelocity impact.¹⁸⁻²⁰ We cannot write a definite account as to whether contamination goes to
144 the mirror, or to the structure around (including other mirrors). The danger with ejected material
145 is that it can contaminate other components in the system, which, for a given contamination level,
146 can generate a higher scattered light contribution to the photodetectors. In principle, the amount
147 of stray light caused by contamination may be of the same order or even larger than that caused by
148 the impact craters. The mechanisms for redeposition go well beyond the scope of the paper, but we
149 can place upper limits by supposing that the impacted mirror cannot not receive more than 100% of
150 the contamination it generates. So, in this paper, we derive an upper limit for the contamination of
151 the impacted mirror, by considering that all ejected matter is deposited back. After DCD estimates,
152 we give expressions to calculate the total mass ejected for single micrometeoroid impact.

153 *3.2.1 Estimate of the damage crater diameter*

154 To calculate the size of the DCD, we use two different models^{2,21} with seven sets of parameters in
155 total.

156 The Hörz²¹ model is based on the analysis of three laboratory experiments performed by inde-

157 pendent investigators in order to calibrate lunar micro craters. The damage crater diameter D [cm]
 158 is found to be a function of the mass of the projectile m [g]:

$$D = C \times m^\Lambda \quad (1)$$

159 The coefficients C [cm] and Λ are given in table 1. The DCD as function of mass for these three
 160 Hörz models are given in Fig. 2.

Table 1 $\log_{10}C$ and Λ coefficients of the Hörz model²¹ and Eq. 1. Each set of the coefficients corresponds to an independent experiment. These values were obtained with targets made of a glass type material and are relevant for the Zerodur^(R) M1 mirror of the LISA telescope.

	$\log_{10}C$	Λ
Hörz 1	1.569	0.37
Hörz 2	1.793	0.396
Hörz 3	1.485	0.377

161 Another model is based on a damage equation,¹⁶ which describes the physics of projectiles
 162 impacting a target at high velocities. The damage crater diameter D in this case is given by:

$$D [\text{cm}] = K_1 K_c d_\mu^\zeta \rho_\mu^\beta v^\gamma [\cos\alpha]^\xi \rho_t^\kappa, \quad (2)$$

163 where K_1 is a factor characteristic of the model, d_μ [cm] is micrometeoroid diameter, ρ_μ , ρ_t [g/cm³]
 164 are the densities of the micrometeoroid particle and target respectively, v [km/s] is the impact ve-
 165 locity, α is the impact angle, the crater factor K_c is the ratio of the crater radius to the crater depth
 166 and it may be as high as 10 for brittle targets such as Zerodur^(R).¹⁶

167 The origin of the equation parameters is independent investigations (Gault, Fechtig, McHugh&
 168 Richardson, Cour-Palais), which are summarized in the Ref.¹⁶ Typical values of the parameters of

169 the Eq. 2 are given in the Table 2.

Table 2 Parameters for DCD calculation with Eq. 2 in case of brittle targets.¹⁶

Model	K_1	ζ	β	γ	ξ	κ	K_c
Gault	1.08	1.071	0.524	0.714	0.714	-0.5	10
Fechtig	6.0	1.13	0.71	0.755	0.755	-0.5	10
McHugh&Richardson	1.28	1.2	0	2/3	2/3	0.5	10
Cour-Palais	1.06	1.06	0.5	2/3	2/3	0	10

170 As a conservative approach, the value of the impact angle α is set to 0° . In the LISA tele-
171 scope, the material for the primary M1 mirror will be Zerodur^(R) ceramics with a density of
172 $\rho_t = 2.53 \text{ g/cm}^3$. Zerodur^(R) is a brittle material. We assume that the coating on the mirror
173 does not affect crater formation. We choose $K_c = 10$ as the worst-case scenario.

174 The results of the different DCD calculations are given in Fig. 4. The difference between
175 different models (up to one order of magnitude) can be explained by the variety of the experimental
176 conditions in the study of hypervelocity impacts, the complexity of the physical phenomena, and
177 the different analytical approaches of the investigations. We assume that some of the used models
178 may overvalue or undervalue DCD for Zerodur^(R) material. For this reason, we calculate the BRDF
179 and perform optical simulations for each model separately. In the future, new experimental data
180 might help to make a preference between the various models listed above, or possibly new models.

181 3.2.2 Estimate of mass ejection

182 As a micrometeoroid impact is a micro-explosion event, some mass will be ejected and can con-
183 taminate surfaces including the M1 mirror. Here we consider this micro-explosion process and
184 calculate the total amount of ejected mass M_e .

185 To calculate M_e , we use the equation derived by Gault^{18,19} following the analysis of a range of

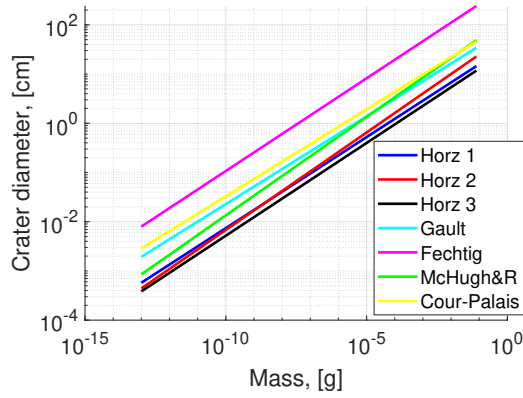


Fig 4 Calculated DCD with models listed above for micrometeoroids of mass $10^{-13} - 10^{-2}$ g, impact velocity 20 km/s and micrometeoroid density 2.5 g/cm^2 .

186 experimental data:

$$M_e = 7.41 \times 10^{-6} K (\rho_\mu / \rho_t)^{1/2} E_i^{1.133} (\cos \alpha)^2 \text{ (SI units)}, \quad (3)$$

187 where E_i – is the projectile kinetic energy in Joule, and α – is the angle of impact. For brittle
 188 materials such as Zerodur^(R), the coefficient K depends on the diameter d_μ of the micrometeoroid:
 189 $K = 1$ for $d_\mu > 10 \text{ }\mu\text{m}$ and otherwise $K = d_\mu \text{ [m]} / 10^{-5}$.

190 To derive a worst-case value, we assume that all the ejected mass will be deposited on the M1
 191 mirror surface. As a result, using Eq. 3, we can calculate the mass ejected for each mass of the
 192 micrometeoroid and so to build an appropriate M1 contamination model (see Sec. 3.3.2).

193 3.3 BSDF Calculations

194 As was mentioned above, the hypervelocity impact of the mirror surface by a micrometeoroid can
 195 cause scattering for two reasons: from the impact crater and ejected contamination. Each of them
 196 requires a specific analysis.

197 3.3.1 BSDF due to crater damage

198 To calculate $BSDF(\theta)$ (θ is the scattering angle) from damage craters, we use the Peterson model,
199 which is devoted to calculating the BSDF of the scattering due to digs in optical components.⁴
200 We assume that modelling the scattering from a dig can apply to modelling the scattering from an
201 impact crater of the same diameter. In this model for a crater of a given diameter D , the scattered
202 light is divided into two contributions:

- 203 • "geometric" scattering or backscattering from surfaces inside the crater, considered as a
204 Lambertian scatterer of diameter D

- 205 • diffraction of light that passes around the crater, considered as a circular mask of diameter
206 D .

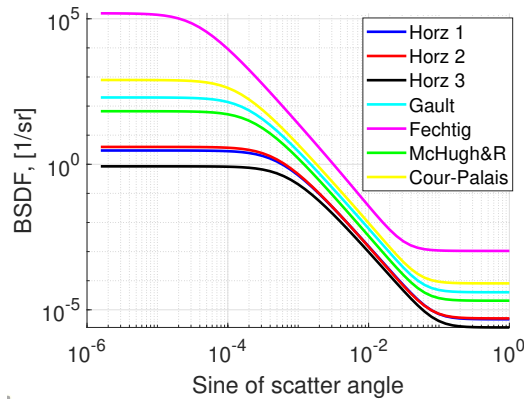


Fig 5 Application of the Peterson model⁴ to the scattering from a surface damaged by micrometeoroids. Assumptions: exposition duration is four years, exposition area is a disk with a diameter of 30 cm, micrometeoroid flux is given by the Grün model.¹⁵ The names given to the BSDF models are the same as the ones used in Sec. 3.2.1 in the calculation of the DCD.

207 In the Peterson model⁴ the digs are considered to be circular, and the intensity of diffracted
208 light from a dig (crater) is calculated using scalar diffraction theory in the Fraunhofer (far-field)

209 limit and Babinet’s principle. So, the total BSDF from digs (craters) is calculated as the sum of the
 210 geometric and diffraction contributions:

$$BSDF(\theta) = \frac{N_D D^2}{4} \times \left[1 + \frac{\pi^2 D^2}{4\lambda^2} \left(1 + \frac{\sin^2(\theta)}{l_D^2} \right)^{-3/2} \right], \quad (4)$$

211 where N_D is the number of digs per unit area, D is dig (crater) diameter, $\lambda = 1.064 \mu\text{m}$ is optical
 212 wavelength, and the roll-off angle⁴ is $l_D = \left(\frac{4}{\pi^4}\right)^{\frac{1}{3}} \frac{\lambda}{D}$. After integration over the range of microm-
 213eteorite masses, the calculated BSDF for different models of DCD is given in Fig. 5. We further
 214 proceed with FRED optical software in which the ”ABg model” of BSDF is embedded. This model
 215 is widely used to describe scattering due to microroughness^{10,22} and involves only three paramete-
 216rs: A , B , and g corresponding, respectively to a proportionality factor, to a roll-of angle, and to
 217 a slope. To implement this Peterson model in the FRED software, we fit the resulting BRDF (see
 218 Fig. 5) with the ABg model plus a constant term:

$$BSDF = \frac{A}{B + (\sin(\theta))^g} + \frac{R}{\pi} \quad (5)$$

219 The first term in Eq. 5 corresponds to the diffraction of light that passes around the crater, and
 220 the second term corresponds to Lambertian scattering of level R inside the crater. The fit of the
 221 Peterson BSDF by the ABg model²² curve was previously used to simulate light scattering by digs
 222 in the METIS coronagraph.²³

223 Let us now consider backscattering from the primary mirror of NASA’s model of the LISA
 224 telescope. The precalculated BSDF for different models of DCD is shown in Fig. 5. The con-
 225 tribution to the backscattering fraction due to the diffractive part varies according to the different

226 models from 1.6% to 8.7% (5.4% on average over the seven models). All the rest is due to Lam-
 227 bertian scattering. So in this particular case, methods based on percentage area coverage¹⁰ give a
 228 reasonable estimate of the scattered light due to micrometeoroid damage.

229 The total integrated scatter (TIS) is a ratio of the total scattered power to the incident power.
 230 TIS for different models and mission duration is given in Table 3. The values of TIS due to
 231 micrometeoroid damage is significant.

Table 3 Total integrated scatter for the nominal and extended mission duration^{16,21}

Model	TIS, 4 years	TIS, 10 years
Hörz 1	2.35×10^{-5}	9.02×10^{-5}
Hörz 2	2.52×10^{-5}	1.02×10^{-4}
Hörz 3	1.23×10^{-5}	4.79×10^{-5}
Gault	2×10^{-4}	7.44×10^{-4}
Fechtig	5.26×10^{-3}	2.05×10^{-2}
McHugh&Richardson	1.03×10^{-4}	4.2×10^{-4}
Cour-Palais	4.04×10^{-4}	1.49×10^{-3}

232 The variations of the computed TIS values are large. Presently there is no preferable model, so
 233 we used all available models, from the most pessimistic to the most optimistic. Further work on
 234 this topic is required to distinguish the best model to use.

235 3.3.2 BSDF due to ejected contamination

236 To calculate the BSDF due to ejected contamination, we assume that the size distribution of parti-
 237 cles can be described with the (IEST)CC1246 standard.²⁴ It describes the number of particles N_p
 238 (per 0.1 m²) whose diameter is greater than or equal to D_p by:

$$N_p(S, CL, D_p) = 10^{|S|[\log_{10}^2(CL) - \log_{10}^2(D_p)]}, \quad (6)$$

239 where S is the slope of particle size distribution, CL is the cleanliness level, D_p is particle diameter
240 in μm .

241 This is a common way to describe the distribution of the contamination on an optical surface.
242 The model is implemented in FRED optical software and is easy to use as it requires only a few
243 parameters (λ , S , CL , etc.) and relies on the properties of Mie scattering. Here we will calculate
244 the cleanliness level using the definition of the CL parameter (the largest particle [in microns],
245 which can be found on a surface of 0.1 m^2 ; see Eq. 6) and using the following considerations:

- 246 • In the regime of hypervelocity micrometeoroid impacts, the largest ejected particle mass is
247 reported to be proportional to the total mass ejected.²⁰ For simplification, we assume the
248 worst case when the coefficient of proportionality is equal to one: the biggest ejecta carries
249 most of the ejected mass and there cannot be a particle more massive than total ejected mass.
250 As a consequence, the biggest mass ejected is from the biggest impact micrometeoroid. This
251 assumption is made for only the largest particle on the surface. The distribution of ejected
252 particles is assumed to be given by the (IEST)CC1246 standard.
- 253 • Ejected mass is mainly target mass (Zerodur^(R)) and has the same density as target material.
254 Ejected particles are spherical.
- 255 • All the ejected mass deposits back onto the surface.

256 Using the flux calculated in Sec. 3.1 and ejected mass in 3.2.2, we find that after four years of
257 exposition, we will have maximum ejected mass equal to $1.14 \times 10^{-4} \text{ g}$, which corresponds to a
258 diameter of a sphere equal to $441 \mu\text{m}$, so $CL = 441$.

259 To find the slope S , we use the mass conservation law. The total mass of particles, which is

260 given by this distribution, should be equal to the total mass ejected over the exposition duration:

$$\sum_{D_p=0}^{\infty} \Delta \left(N_p(S, CL, D_p) \right) \frac{S_m}{0.1 \text{ [m}^2]} \times m(D_p) = \sum_{d_\mu=0}^{\infty} M_e(d_\mu) \times \Delta \left(\phi_G(m(d_\mu)) \right), \quad (7)$$

261 where S_m is the M1 mirror area, the mass of the micrometeoroid $m(x)$ is a function of its equivalent
 262 sphere diameter x and M_e is the ejected mass given in the Sec. 3.2.2, $\phi_G(m)$ is integrated flux given
 263 in Sec. 3.1, Δ is a difference operation between the neighboring bins of the distribution (N_p and
 264 ϕ_G are cumulative distributions). On the right side of Eq. 7 is the total mass ejected due to all
 265 micrometeoroid impacts, and in the left side is the total mass of contaminations, assuming that
 266 the distribution of particles on the surface will be given by Eq. 6. When the slope parameter S is
 267 chosen correctly, these two masses will be equal.

268 We find that for four years, the absolute value of the slope is equal to $S = 0.8738$, which is quite
 269 close to the value 0.926 used in the CC1246D standard. For ten years of exposition: $CL = 743.2$
 270 and $S = 0.7668$.

271 Up until this point we have ignored the silver coating of the Zerodur^(R) mirror. We have
 272 assumed that only Zerodur^(R) material is ejected. However, we can also assume that the silver
 273 coating will play a role in the amount of ejected mass, so in the limiting case we assume that
 274 only silver will be ejected. We consider this case only for the mass ejection calculation. In all
 275 other cases only uncoated Zerodur^(R) material is considered. In this case in Eq. 3 the coefficient
 276 is $K = 1$ for all diameters of the micrometeoroid. The corresponding S and CL coefficients are
 277 $S = 1.2827$ and $CL = 216.6$ for four years of mission duration and $S = 1.0998$, $CL = 365$ for
 278 ten years.

279 *3.4 FRED Simulations*

280 The backscattering in the direction of the photodiode of the LISA telescope has been calculated
281 using the FRED simulation software. The scattering model has been applied for the M1 telescope
282 mirror only. The scattering calculation includes two main items: due to impact craters and due to
283 ejected mass contamination.

284 *3.4.1 Scattering due to impact craters*

285 To calculate scattering due to impact craters in FRED software, we use two embedded BSDF
286 models: Lambertian and ABg. The coefficients of these models were obtained from the fit of total
287 Peterson’s BSDF, as was described in section 3.3.1. The calculation results are summarized in the
Tab. 4. Despite the high values of the TIS (see Tab. 3), the values of backscattering are low, as the

Table 4 Backscattering fraction (BSF) for the nominal and extended mission duration in the LISA telescope

Model	BSF, 4 years	BSF, 10 years
Hörz 1	3.2e-15	1.2e-14
Hörz 2	3.4e-15	1.1e-14
Hörz 3	1.7e-15	6.4e-15
Gault	2.6e-14	9.5e-14
Fechtig	6.6e-13	2.5e-12
McHugh&Richardson	1.3e-14	5.4e-14
Cour-Palais	5.2e-14	1.9e-13

288
289 coupling factor of the M1 mirror is low.

290 To study the impact of micrometeoroid parameters on the final result, we consider a situation
291 when the density of micrometeoroid follows the step distribution given in Fig. 2 (blue curve), and
292 we simulate distribution velocities following Taylor’s¹⁷ observations, which is a re-evaluation of
293 the Harvard Radio Meteor Project data of about 20000 meteor observations. The result is summa-
294 rized in Table 5 (third column). For comparison, the second column contains values of backscat-

295 tering fraction with the assumptions used in the paper: constant velocity $v = 20$ km/s and density
 296 $= 2.5$ g/cm³ of the micrometeoroid. No qualitative change is observed. The values are slightly
 lower, as the considered density of micrometeoroids is lower.

Table 5 Backscattering fraction for variable density and velocity of the micrometeoroids.

Model	BSF, 4 years Constant ρ, V	BSF, 4 years Variable ρ, V
Gault	2.6e-14	1.7e-14
Fechtig	6.6e-13	5.1e-13
McHugh&Richardson	1.3e-14	1.4e-14
Cour-Palais	5.2e-14	3.7e-14

297

298 The FRED divot analysis approach was used by NASA²⁵ to estimate micrometeoroid damage
 299 of the M1 mirror. In their work, the total area occupied by the crater was modeled as a single divot
 300 placed on the M1 mirror surface. Depending on the position of the divot on the mirror surface, the
 301 BSF obtained in their study is in range from 1.73e-14 to 3.33e-13, which is compatible with the
 302 values obtained in this study.

303 3.4.2 Scattering due to ejected mass contamination

304 The FRED calculation of contamination was performed with the embedded 1246C²⁴ standard. The
 305 values of CL and S used in the simulation are listed in the section 3.3.2. The computed values of
 306 backscattering are summarised in Tab. 6. As Zerodur^(R) mirror will be coated with silver, it would
 307 certainly cause an effect of contamination population, and so the real value of scattering will be in
 308 between two limit cases: mirror material is only Zerodur^(R) and mirror material in only silver.

309 These values are compatible with the highest of the scattering data of Table 4 (6.6e-13 for 4
 310 years and 2.5e-12 for 10 years). So scattering contribution due to ejected mass is dominant under

Table 6 Backscattering fraction due to contamination for four and ten years mission duration.

Mirror material	BSF, 4 years	BSF, 10 years
Zerodur ^(R)	4.93e-13	1.04e-12
Silver	2.16e-12	4.46e-12

311 the assumption that 100% of the ejecta contribute to the M1 contamination and should not be
312 neglected in stray-light estimates caused by micrometeoroid impacts.

313 **4 Conclusion**

314 In this paper, we developed a method for the estimation of the stray-light due to micrometeoroid
315 damage of optical surfaces. It consists of four steps. The first step is the flux calculation based
316 on the satellite environmental model. The second step is the calculation of the damage crater
317 diameter and ejected mass. The third step is the calculation of the corresponding bidirectional
318 reflectance distribution function using the Peterson model and the 1246C standard. The last step
319 is the calculation of the scattering with an optical software, for the detailed application to the
320 considered optical configuration. We have applied the method to the simulation of the scattering of
321 light in the LISA telescope, due to the damage to the primary mirror from micrometeoroid impact.
322 The results suggest that even under the worst-case assumptions the impact craters and the resulting
323 contamination contribute to an acceptable scattering of light to the LISA detectors.

324 It should be noticed that contamination due to mass ejection gives a significant contribution.
325 Further work should address possible contamination due to ejecta towards mirrors other than the
326 primary mirror.

327 The main sources of uncertainty are in the modelling of the damage crater diameter and in
328 the distribution of ejected particles (shape and quantity) on the damaged surface. The modelling

329 presented here should benefit from any future improvements in the experimental data, particularly
330 when optical materials are used as targets for the hypervelocity impact experiments.

331 The method is straightforward to apply, to modify, and it can be used for any space optical
332 instrument with minor parameter changes. The code is available on GitHub.²⁶ The model can
333 be used not only for reflective but for refractive optics as well. The final result of the scattered
334 light calculation depends on the optical design of the telescope, in our case the beam expanding
335 telescope that is required to transmit the emitted beam to the distant spacecraft.

336 *Acknowledgments*

337 We thank CNES for funding this research. We thank Photon Engineering for providing the uni-
338 versity FRED Optical Engineering Software license. The authors thank their colleagues in the
339 LISA Consortium Straylight Working Group. Also, we would like to acknowledge Région Sud
340 and Thales Alenia Space for the funding of the thesis work of Vitalii Khodnevykh.

341 *References*

- 342 1 B. G. Cour-Palais, "Meteoroid environment model-1969," NASA-SP-8013 (1969).
- 343 2 J. B. Heaney, "MLCD micrometeoroid optical damage analysis – solar window," unpublished
344 (2005).
- 345 3 P. Lightsey, C. Atkinson, M. Clampin, et al., "James webb space telescope: Large deployable
346 cryogenic telescope in space," Optical Engineering **51**, 1003– (2012).
- 347 4 G. Peterson, "A BRDF model for scratches and digs," Proceedings of SPIE - The International
348 Society for Optical Engineering **8495** (2012).

349
350
351
352
353
354
355
356
357
358
359
360
361
362
363
364
365
366
367
368
369

5 “LISA Mission Proposal for L3 submitted to ESA,
<https://www.lisamission.org/?q=articles/lisa-mission/lisa-mission-proposal-l3>,” (2017).

6 A. Einstein, “Näherungsweise integration der feldgleichungen der gravitation,”
Sitzungsberichte der Königlich Preussischen Akademie der Wissenschaften , 688–696
(1916).

7 B. P. Abbott, R. Abbott, T. D. Abbott, et al., “Observation of gravitational waves from a
binary black hole merger,” Phys. Rev. Lett. **116**, 061102 (2016).

8 Einstein Gravitational Wave Telescope Conceptual Design Study: ET-0106C-10 (2011).

9 <https://beta.sam.gov/opp/72d6f9eaf7308681d44a4391e73ad57b/view?keywords=80GSFC19R0032&sort=-1>

10 E. Fest, Stray light analysis and control, SPIE Press (2013).

11 <https://photonengr.com/fred-software/>.

12 <https://www.zemax.com/>.

13 <https://www.synopsys.com/optical-solutions/codev.html>.

14 M. Millinger and P. Jiggins, “LISA Environment Specification,” ESA-L3-EST-MIS-SP-001,
ESA-TEC-SP-006666, (unpublished) (2017).

15 E. Grün, H. Zook, H. Fechtig, et al., “Collisional balance of the meteoritic complex,” Icarus
62(2), 244 – 272 (1985).

16 ESA’s Space Environment Information System’s webpage
<https://www.spennis.oma.be/help/background/metdeb/metdeb.html#METFLUX>.

17 A. Taylor, “The Harvard Radio Meteor Project Meteor Velocity Distribution Reappraised,”
Icarus **116**(1), 154 – 158 (1995).

- 370 18 D. Gault, “Displaced mass, depth, diameter, and effects of oblique trajectories for impact
371 craters formed in dense crystalline rocks,” The Moon **6**, 32–44 (1973).
- 372 19 J.-M. Siguier and J.-C. Mandeville, “Test procedures to evaluate spacecraft materials ejecta
373 upon hypervelocity impact,” Proceedings of The Institution of Mechanical Engineers Part
374 G-journal of Aerospace Engineering - PROC INST MECH ENG G-J A E **221**, 969–974
375 (2007).
- 376 20 J. O’Keefe and T. Ahrens, “The size distribution of fragments ejected at a given velocity from
377 impact craters,” International Journal of Impact Engineering **5**, 493–499 (1987).
- 378 21 F. Hörz, D. Brownlee, H. Fechtig, et al., “Lunar microcraters: Implications for the microme-
379 teoroid complex,” Planetary and Space Science **23**(1), 151 – 172 (1975).
- 380 22 R. Pfisterer, “Approximated scatter models for: Stray light analysis,” OPN Optics &
381 Photonics News , 16–17 (2011).
- 382 23 S. Fineschi, P. Sandri, F. Landini, et al., “Stray-light analyses of the METIS coronagraph
383 on Solar Orbiter,” in Solar Physics and Space Weather Instrumentation VI, S. Fineschi and
384 J. Fennelly, Eds., International Society for Optics and Photonics, SPIE (2015).
- 385 24 Product cleanliness levels and contamination control program, Military Standard (MIL STD)
386 1246C, U.S. Department of Defense, Washington, DC (1994).
- 387 25 L. Seals, “FRED Divot Analysis,” (unpublished technical note) (2019).
- 388 26 <https://github.com/KVital/BSDF>.

389 List of Figures

- 390 1 Schema of the Cassegrain four mirror telescope designed by NASA for the LISA
391 mission. The same telescope is used to expand the transmitted beam and collect
392 the light of the received beam.
- 393 2 The Grün meteoroid flux-mass model (in black) and the step function of density
394 distribution (in blue)¹⁶
- 395 3 The expected number of micrometeoroid impacts on the M1 mirror, calculated
396 according to the Grün Model, as a function of the micrometeoroid mass. The bin
397 size is logarithmically uniform. The total number of micrometeoroid impacts with
398 mass $> 1 \times 10^{-12}$ g is 92 for four years mission and 231 for ten years mission.
- 399 4 Calculated DCD with models listed above for micrometeoroids of mass 10^{-13} –
400 10^{-2} g, impact velocity 20 km/s and micrometeoroid density 2.5 g/cm².
- 401 5 Application of the Peterson model⁴ to the scattering from a surface damaged by
402 micrometeoroids. Assumptions: exposition duration is four years, exposition area
403 is a disk with a diameter of 30 cm, micrometeoroid flux is given by the Grün
404 model.¹⁵ The names given to the BSDF models are the same as the ones used in
405 Sec. 3.2.1 in the calculation of the DCD.

406 **List of Tables**

- 407 1 $\log_{10}C$ and Λ coefficients of the Hörz model²¹ and Eq. 1. Each set of the coeffi-
408 cients corresponds to an independent experiment. These values were obtained with
409 targets made of a glass type material and are relevant for the Zerodur^(R) M1 mirror
410 of the LISA telescope.
- 411 2 Parameters for DCD calculation with Eq. 2 in case of brittle targets.¹⁶
- 412 3 Total integrated scatter for the nominal and extended mission duration^{16,21}
- 413 4 Backscattering fraction (BSF) for the nominal and extended mission duration in
414 the LISA telescope
- 415 5 Backscattering fraction for variable density and velocity of the micrometeoroids.
- 416 6 Backscattering fraction due to contamination for four and ten years mission dura-
417 tion.